Development and validation of a deep learning system to classify aetiology and predict anatomical outcomes of macular hole

Yu Xiao [1,2] Yijun Hu [3,4] Wuxiu Quan,[5] Yahan Yang,[6] Weiyi Lai,[6] Xun Wang,[6] Xiayin Zhang,[6] Bin Zhang,[5] Yuqing Wu,[6] Qiaowei Wu [1,2] Baoyi Liu,[1,2] Xiaomin Zeng,[1,2] Zhanjie Lin,[1] Ying Fang,[1] Yu Hu,[7] Songfu Feng,[8] Ling Yuan,[7] Hongmin Cai,[5] Tao Li [6] Haotian Lin [6,9] Honghua Yu [1,2]

ABSTRACT

Aims To develop a deep learning (DL) model for automatic classification of macular hole (MH) aetiology (idiopathic or secondary), and a multimodal deep fusion network (MDFN) model for reliable prediction of MH status (closed or open) at 1 month after vitrectomy and internal limiting membrane peeling (VILMP).

Methods In this multicentre retrospective cohort study, a total of 330 MH eyes with 1082 optical coherence tomography (OCT) images and 3300 clinical data enrolled from four ophthalmic centres were used to train, validate and externally test the DL and MDFN models. 266 eyes from three centres were randomly split by eye-level into a training set (80%) and a validation set (20%). In the external testing dataset, 64 eyes were included from the remaining centre. All eyes underwent macular OCT scanning at baseline and 1 month after VILMP. The area under the receiver operated characteristic curve (AUC), accuracy, specificity and sensitivity were used to evaluate the performance of the models.

Results In the external testing set, the AUC, accuracy, specificity and sensitivity of the MH aetiology classification model were 0.965, 0.950, 0.870 and 0.938, respectively; the AUC, accuracy, specificity and sensitivity of the postoperative MH status prediction model were 0.904, 0.825, 0.977 and 0.766, respectively; the AUC, accuracy, specificity and sensitivity of the postoperative idiopathic MH status prediction model were 0.947, 0.875, 0.815 and 0.979, respectively.

Conclusion Our DL-based models can accurately classify the MH aetiology and predict the MH status after VILMP. These models would help ophthalmologists in diagnosis and surgical planning of MH.

INTRODUCTION

Macular hole (MH), a full-thickness defect of the neurosensory retina tissue at the fovea, is one of the reasons for central vision deterioration.[1] MH can be divided into two categories according to the aetiology. The aetiology of idiopathic MH (IMH) is unknown, while secondary MH (SMH) is caused by known aetiologies like high myopia and trauma. IMH is the most common type of MH. It is estimated to affect 0.1%–0.8% of the population aged over 44 years, and nearly two-thirds of patients with IMH are female.[2–4] IMH development is considered as pathological vitreoretinal traction at the central macula.[5] Patients with IMH with progressive visual impairment and metamorphopsia usually require surgical intervention.[6] Vitrectomy and internal limiting membrane peeling (VILMP) has been proved effective to treat full-thickness IMH with success rates of 80%–95%.[7 8] However, IMH remains open after routine VILMP in some cases.[9] For instance, it was reported that up to 44% of large MHs remained open after first surgery.[10] In patients with an open IMH after initial surgery, a second surgery is often mandatory.[11] However, second surgery is typically associated with higher medical costs and less promising visual outcomes.[9] SMH is usually caused by high myopia and blunt ocular trauma.[12 13] The pathogenesis of SMH is more complicated and the success rate of initial repair is lower than that of IMH.[12 14] Therefore, it is important to distinguish IMH and SMH, and to predict the postoperative MH status after initial repair during surgical planning.

Optical coherence tomography (OCT) has been widely used in diagnosis and prognosis assessment of MH.[13 15] IMH may have different OCT images from SMH, especially those secondary to high myopia, with its own OCT characteristics.[12] For prognosis assessment, some OCT parameters have been identified as factors related to outcomes of MH surgeries. These factors include the minimum diameter of MH (MIN), the base diameter of MH (BASE), hole form factor (HFF), macular hole index (MHI), tractional hole index (THI) and diameter hole index (DHI).[12 13 16–19] However, many previous studies mainly focused on the prediction abilities of one OCT parameter only.[15]

Deep learning (DL) is an emerging artificial intelligence technology, which has been successfully applied in various areas, such as image identification and classification.[20 21] Convolutional neural network (CNN), one of the most popular DL models, employs multiple convolutional layers for automatic identification and extraction of feature representations. A CNN-based DL model was recently developed to automatically detect IMH using ultra-wide-field fundus images.[22] In addition to the CNN, the multimodal deep fusion network (MDFN) is an important technology to exploit the comprehensive information of multimodal data

extracted by different unimodal DL models. Different feature sets of the multimodal data can be fused by MDFN to improve the performance of the DL model.[23] Given the fact that the surgical outcome of MH is affected by both morphological factors (such as preoperative macular OCT parameters) and other clinical factors (such as duration of MH), MDFN is potentially helpful in the prediction of postoperative MH status by combining the information of these factors.

The current study aimed to develop a DL model for automatic classification of MH aetiology based on macular OCT images, and an MDFN-based DL model to automatically predict MH status after VILMP surgery using preoperative OCT images and other clinical data. We also compared the performance of the MDFN model with that of the unimodal models.

METHODS

Participants and data collection

In this multicentre retrospective cohort study, eyes with full-thickness MH (ie, IMH and SMH caused by high myopia or trauma) followed up for at least 1 month after VILMP surgery were included. The surgical process of VILMP is described in the online supplemental eMethod 1. The patients' age, gender and duration of symptoms (eg, progressive visual impairment and metamorphopsia) were extracted from the electronic medical records (EMR). All of the eyes underwent ophthalmologic examinations including slit-lamp biomicroscope anterior segment and fundus examination, and spectral domain-OCT scanning (SD-OCT, Spectralis; Heidelberg Engineering, Heidelberg, Germany) at baseline and 1 month after VILMP. Additional details on OCT examination and OCT parameter measurements are presented in the online supplemental eMethod 2.

MH eyes were recruited retrospectively between January 2014 and August 2020. Among the 349 MH eyes of 334 patients with 1125 preoperative macular OCT images received from four ophthalmic settings, 5 eyes were excluded due to missing preoperative OCT images, 8 eyes were excluded due to missing postoperative OCT images and 6 eyes were excluded due to insufficient quality of OCT images. The remaining 330 eyes of 315 patients with 1082 preoperative macular OCT images (285 IMH eyes with 957 images and 45 SMH eyes with 125 images (36 eyes with 106 images secondary to high myopia, 9 eyes with 19 images secondary to trauma)) and 3300 clinical data (preoperative macular OCT parameters extracted from the OCT device and clinical data from EMR) were used to train, validate and externally test the MH aetiology classification model and postoperative MH/IMH status prediction model. Of these eyes, 266 MH eyes (232 IMH eyes and 34 SMH eyes) collected from the Zhongshan Ophthalmic Center, the Department of Ophthalmology in the Zhujiang Hospital of Southern Medical University and the Department of Ophthalmology in the First Affiliated Hospital of Kunming Medical University were randomly divided into the training set (80% of the eyes) and the validation set (the other 20% of the eyes). A separate set of 64 MH eyes (53 IMH eyes and 11 SMH eyes) collected from the Department of Ophthalmology in the Guangdong Provincial People's Hospital was used for external testing. The flow chart of the research performed in this study is shown in figure 1.

Development of DL model for MH aetiology classification

The Visual Geometry Group network (VGG, Department of Engineering Science, The University of Oxford, Oxford, UK) with 16 convolutional layers was employed for the classification of MH aetiology.[24] Preoperative macular OCT images were used
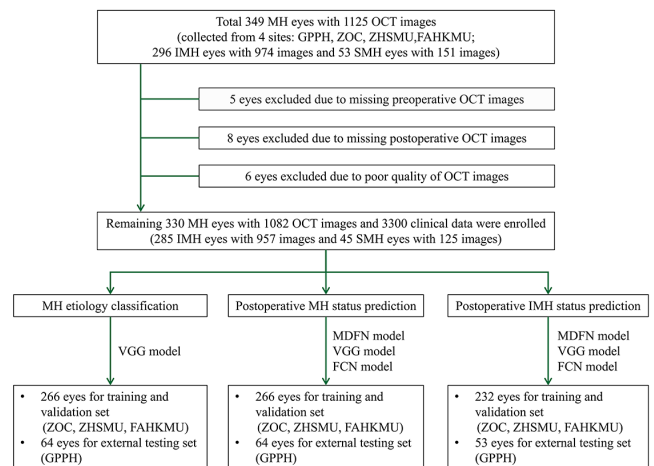

Figure 1 Flow chart of the research performed in this study. FAHKMU, First Affiliated Hospital of Kunming Medical University; FCN, fully connected network; GPPH, Guangdong Provincial People's Hospital; IMH, idiopathic macular hole; MDFN, multimodal deep fusion network; MH, macular hole; OCT, optical coherence tomography; SMH, secondary macular hole; VGG, Visual Geometry Group; ZHSMU, Zhujiang Hospital of Southern Medical University; ZOC, Zhongshan Ophthalmic Center.

as the input data. Based on the requirements of VGG network, the OCT images were preprocessed to normalise the input data. We removed saturated pixels from the raw OCT images with an intensity value of 255, followed by resizing them into 224×224 pixels. A threshold probability value of 0.5 was used to classify the MH aetiology (ie, SMH if the value was 0.5 or more, or IMH if the value was <0.5) (figure 2). A detailed description of MH aetiology labelling and training procedure is described in the online supplemental eMethod 3.

Development of DL models for MH/IMH status prediction

Considering that the pathogenesis of SMH is more complicated and the success rate of initial repair is even lower than IMH, two prediction tasks were performed. For the first prediction task, all of the 330 MH eyes, including both 45 SMH eyes and 285 IMH eyes, were included to predict the postoperative MH status. For the second prediction task, only 285 IMH eyes were enrolled to predict the postoperative status of IMH.

Preoperative macular OCT images and clinical data (ie, age, gender, duration of symptoms, MIN, BASE, height of hole, MHI, HFF, DHI and THI) of MH/IMH eyes were used as the input data. The DL model used for MH aetiology classification (VGG network) was also applied to obtain deep features of OCT images for MH/IMH status prediction. In addition, the fully connected (FC) network was employed to obtain deep features of the clinical data.

After the two types of feature sets (multimodal deep features) were extracted, the VGG network, with the top output layer removed, was connected to the FC network. Moreover, the multimodal deep features were fused to have a comprehensive characterisation of MH/IMH. The concatenate operation could integrate semantic data obtained from diverse feature maps, thereby increasing the number of channels and improving model performance. The fused features were linked to a two-channel softmax layer via the FC layer, to arrive at the predictive probability value of MH/IMH status. A threshold probability value of 0.5 was used to predict MH/IMH status (ie, closed if the value
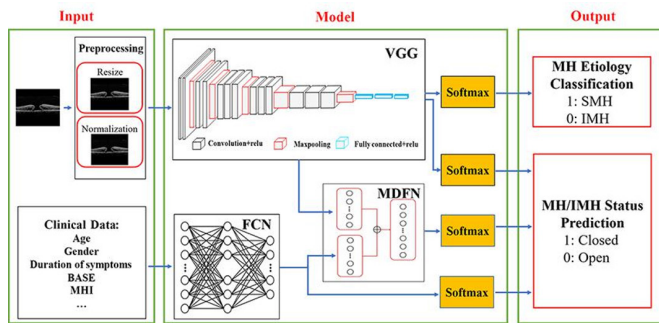
Figure 2 Demonstration of construction of deep learning models. BASE, base diameter of MH; FCN, fully connected network; IMH, idiopathic macular hole; MDFN, multimodal deep fusion network; MHI, macular hole index; MH, macular hole; SMH, secondary macular hole; VGG, Visual Geometry Group. The deep learning models were trained to classify the MH aetiology (ie, SMH or IMH), and to predict postoperative MH/IMH status (ie, closed or open) following initial repair.

was 0.5 or more, or open if the value was <0.5). A detailed description of postoperative MH status labelling and training procedure is given in the online supplemental eMethod 4.

To compare the predictive performance of the MDFN model to those of the unimodal DL models, we divided the MDFN model into two unimodal DL models with the same structure of VGG network and FC network. We first used the VGG network and the FC network to extract deep features of OCT images and clinical data, respectively. Then the MH/IMH status was predicted by the unimodal DL models via the softmax layer.

Schematic illustration of the DL models is presented in figure 2. Statistical analysis is demonstrated in the online supplemental eMethod 5. In addition, we generated heatmaps to aid interpretation of the results and increase model transparency (described in the online supplemental eMethod 6).

RESULTS

Demographic data of the eyes enrolled in this study are summarised in table 1. All patients were of the same ethnicity (Chinese). Among the total 330 MH eyes, 217 eyes were from female patients (66%), and the mean age of patients was 59.54±11.03 years. There were 229 eyes with a closed MH (209 IMH and 20 SMH) and 101 eyes with an open MH (76 IMH and 25 SMH) at the 1-month visit.

The performance metrics and the ROC curves of DL models are shown in table 2 and figure 3, respectively. The confusion matrices for external testing set are presented in the online supplemental eResult 1. For MH aetiology classification, the AUC of the DL model in the training set was 1.000, with an accuracy of 0.998, specificity of 1.000 and sensitivity of 1.000. In the validation set, the DL model showed an AUC of 0.997, with an accuracy of 0.986, specificity of 0.994 and sensitivity of 0.964. In the external testing set, the AUC, accuracy, specificity and sensitivity were 0.965, 0.950, 0.870 and 0.938, respectively (table 2A and figure 3A).

For postoperative MH status prediction, the AUC of the MDFN model in the training set was 0.928, with an accuracy of 0.855, specificity of 0.897 and sensitivity of 0.808. In the validation set, the AUC, accuracy, specificity and sensitivity of the MDFN model were 0.881, 0.826, 0.746 and 0.912, respectively.

Table 1 Baseline characteristics of the eyes*

A. Baseline characteristics of MH eyes*	Training set (n=199)	Validation set (n=67)	Testing set (n=64)	All eyes (n=330)
Aetiology, IMH, n (%)	173 (86.93%)	59 (88.06%)	53 (82.81%)	285 (86.36%)
Gender, female, n (%)	133 (66.83%)	43 (64.18%)	41 (64.06%)	217 (65.76%)
Age, years	59.30 (10.76)	58.24 (11.76)	61.66 (10.74)	59.54 (11.03)
Duration of symptoms, months	7.28 (11.38)	9.60 (22.88)	7.67 (16.55)	7.83 (15.44)
MIN, μm	437.39 (204.75)	484.88 (192.94)	436.05 (238.46)	446.77 (210.32)
BASE, μm	955.78 (460.20)	1004.75 (343.57)	977.34 (429.57)	969.91 (433.41)
Height, μm	439.37 (91.80)	464.66 (102.91)	467.69 (124.10)	449.99 (101.94)
THI	1.50 (2.44)	1.24 (1.03)	2.07 (2.42)	1.56 (2.24)
DHI	0.48 (0.16)	0.49 (0.13)	0.45 (0.18)	0.48 (0.16)
MHI	0.59 (0.43)	0.57 (0.50)	0.68 (0.70)	0.60 (0.51)
HFF	0.77 (0.22)	0.76 (0.16)	0.88 (0.36)	0.79 (0.25)
B. Baseline characteristics of IMH eyes*	Training set (n=174)	Validation set (n=58)	Testing set (n=53)	All eyes (n=285)
Gender, female, n (%)	113 (64.94%)	38 (65.52%)	35 (66.04%)	186 (65.26%)
Age, years	59.36 (11.27)	60.67 (9.33)	63.77 (8.96)	60.45 (10.63)
Duration of symptoms, months	7.18 (11.60)	6.77 (11.04)	7.35 (16.53)	7.13 (12.56)
MIN, μm	453.85 (198.63)	434.71 (214.21)	413.11 (238.00)	442.38 (210.27)
BASE, μm	952.63 (323.98)	884.66 (405.20)	898.34 (391.39)	928.70 (356.23)
Height, μm	447.36 (85.82)	439.97 (89.87)	467.17 (116.15)	449.54 (93.43)
THI	1.45 (2.56)	1.44 (1.16)	2.23 (2.55)	1.59 (2.36)
DHI	0.48 (0.15)	0.52 (0.15)	0.46 (0.19)	0.48 (0.16)
MHI	0.53 (0.25)	0.72 (0.65)	0.75 (0.75)	0.61 (0.49)
HFF	0.75 (0.17)	0.81 (0.28)	0.90 (0.38)	0.79 (0.25)

*Presented with mean (SD) except for aetiology and gender.
BASE, base diameter of MH; DHI, diameter hole index; HFF, hole form factor; IMH, idiopathic macular hole; MH, macular hole; MHI, macular hole index; MIN, minimal diameter of MH; THI, tractional hole index.

Table 2 Performance of the deep learning models

A. Performance of the DL model for MH aetiology classification	AUC	ACC	SPE	SEN
Training	1.000	0.998	1.000	1.000
Validation	0.997	0.986	0.994	0.964
Testing	0.965	0.950	0.870	0.938
B. Performance of the models for postoperative MH status prediction	AUC	ACC	SPE	SEN
MDFN				
Training	0.928	0.855	0.897	0.808
Validation	0.881	0.826	0.746	0.912
Testing	0.904	0.825	0.977	0.766
VGG				
Training	0.953	0.901	0.855	0.922
Validation	0.805	0.778	0.887	0.581
Testing	0.804	0.758	0.872	0.656
FCN				
Training	0.807	0.789	0.759	0.723
Validation	0.776	0.791	0.550	0.936
Testing	0.797	0.813	0.652	0.829
C. Performance of the models for postoperative IMH status prediction	AUC	ACC	SPE	SEN
MDFN				
Training	0.999	0.988	0.989	0.987
Validation	0.974	0.901	1.000	0.865
Testing	0.947	0.875	0.815	0.979
VGG				
Training	0.969	0.901	0.955	0.880
Validation	0.891	0.840	0.782	0.873
Testing	0.836	0.755	0.800	0.762
FCN				
Training	0.873	0.782	0.733	0.876
Validation	0.926	0.828	0.800	0.954
Testing	0.768	0.717	0.625	0.892

ACC, accuracy; AUC, the area under the receiver operating characteristic curve; FCN, fully connected network; IMH, idiopathic macular hole; MDFN, multimodal deep fusion network; MH, macular hole; SEN, sensitivity; SPE, specificity; VGG, Visual Geometry Group.

For external testing, the MDFN model achieved an AUC of 0.904, with an accuracy of 0.825, specificity of 0.977 and sensitivity of 0.766 (table 2B and figure 3B). For IMH status prediction, the AUC of the MDFN model was 0.999 in the training set, with an accuracy of 0.988, specificity of 0.989 and sensitivity of 0.987. In the validation set, the AUC of the MDFN model was 0.974, with an accuracy of 0.901, specificity of 1.000 and sensitivity of 0.865. For external testing, the AUC, accuracy, specificity and sensitivity of the MDFN model were 0.947, 0.875, 0.815 and 0.979, respectively (table 2C and figure 3C). These results indicate that our MDFN models can provide accurate prediction of postoperative MH/IMH status, and the accuracy of the IMH status prediction was slightly higher than that of the MH status prediction.

Additionally, the predictive performance of two unimodal DL models was also evaluated in the external testing set. For MH status prediction, the AUC of VGG network was 0.804, with 0.758 accuracy, 0.872 specificity and 0.656 sensitivity. The AUC

of FC network was 0.797, with 0.813 accuracy, 0.652 specificity and 0.829 sensitivity (table 2B and figure 3D,E). For IMH status prediction, the AUC of VGG network was 0.836, with an accuracy of 0.755, specificity of 0.800 and sensitivity of 0.762. The AUC, accuracy, specificity and sensitivity of FC network were 0.768, 0.717, 0.625 and 0.892, respectively (table 2C and figure 3F,G). These results suggest that performance of the MDFN model was significantly better than those of the unimodal DL models for MH/IMH status prediction.

Heatmaps vividly illustrate the regions most important for decision-making process of the MDFN model (figure 4). In these heatmaps, the gap between the edges of the neuro-retina was identified as the most critical pathological region for prediction of the MH status following VILMP.

DISCUSSION

In this study, we developed a DL model that could accurately distinguish IMH from SMH secondary to high myopia or trauma based on macular OCT images. We also developed an MDFN model capable of precisely predicting the postoperative IMH status based on preoperative macular OCT images and clinical data from a multicentre dataset. Moreover, the prediction accuracy of MDFN model was better than those of unimodal prediction models, suggesting that the MDFN model could improve predictive performance by the integration of image and text features. Furthermore, the prediction accuracy of postoperative status of IMH only was better than that of all MH. This might be due to different prognostic factors between SMH and IMH, and the limited amount of SMH eyes in the study.

MH can be classified into two categories, IMH and SMH caused by known aetiologies such as high myopia and trauma. Treatments for IMH and for SMH caused by high myopia are different. While standard VILMP and gas tamponade is often applied to IMH, SMH due to high myopia usually needs more complicated surgical modalities, such as inverted ILM flap and silicone oil tamponade.[14] Macular OCT images of SMH caused by high myopia are also different from those of the IMH, due to the deformation of the posterior ocular surface.[12] Thus, it is possible to distinguish these two types of MH based on macular OCT images only. In the present study, we further extended the possibility to automatic classification of IMH and SMH. Despite the limited amount of the macular OCT images of SMH, our DL model still achieved an accuracy of 0.965 and an AUC of 0.950 in external testing. This might be resulted from the characteristic features of macular OCT images in eyes with SMH caused by high myopia.

Since IMH is the most common type of MH, it is clinically important to predict the anatomical outcomes of IMH surgeries. Accurate prediction of the postoperative IMH status can alleviate patients' anxieties and help ophthalmologists make better surgical plans. In patients likely to have an unfavourable prognosis after VILMP, more advanced surgical techniques, such as inverted ILM flap and autologous ILM transplantation, can be recommended to the patients.[10 25] OCT imaging is useful in measuring different aspects of IMH morphology with good repeatability and reproduction.[19] Some of the OCT parameters have been used as the prognostic factors of anatomical outcomes after surgery.[17] However, these OCT parameters were evaluated individually in previous studies.[15] The accuracy and universality of these unifactor prediction algorithms are limited, as they only analyse the predictive ability of a single parameter, while the anatomical outcomes of IMH surgery are affected by multiple factors.[4 19] In this study, we propose an MDFN model that
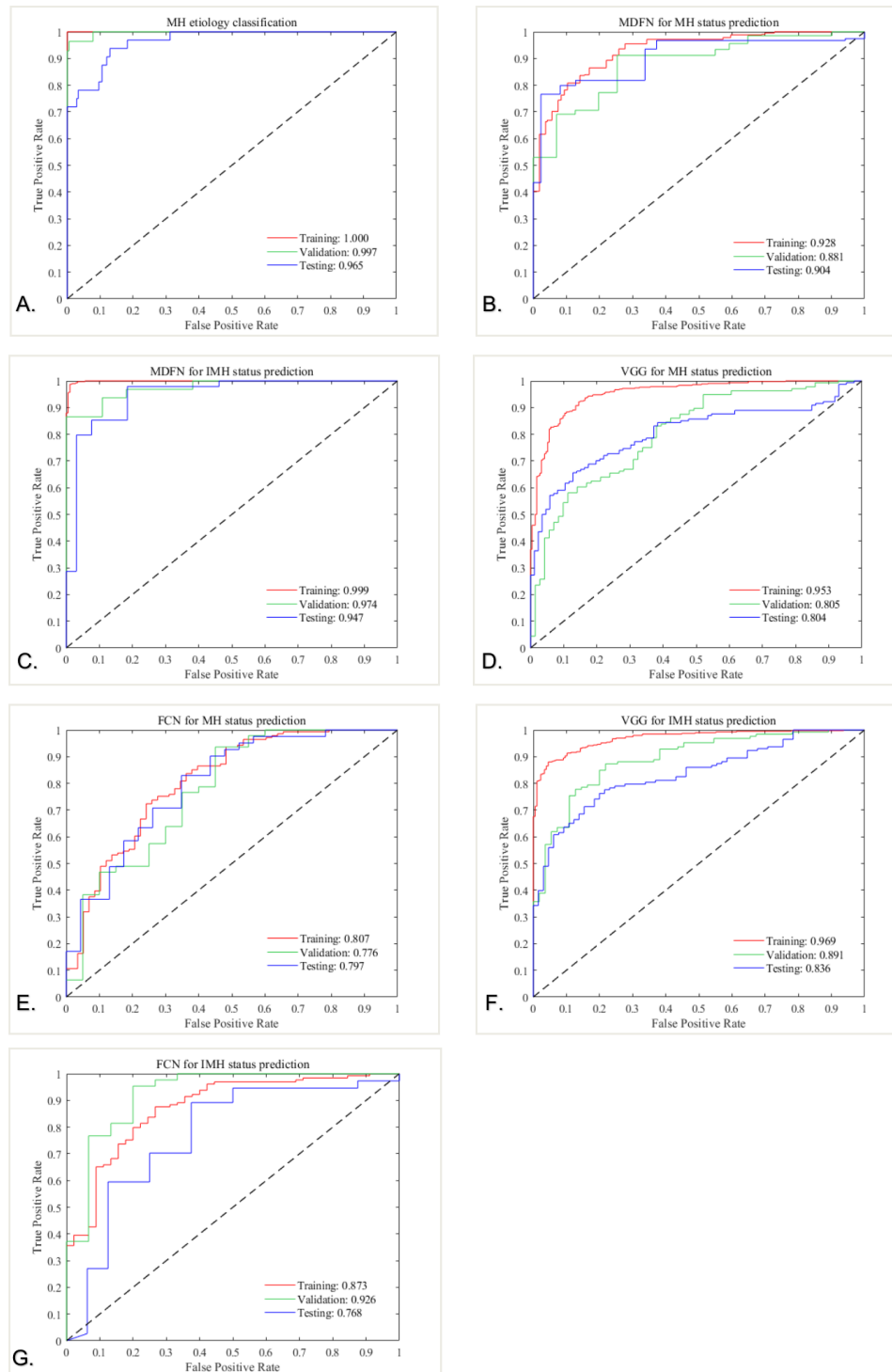
Figure 3 The receiver operating characteristic (ROC) curves of the deep learning models. (A) The ROC curves of the DL model for MH aetiology classification. (B) The ROC curves of the MDFN model for MH status prediction. (C) The ROC curves of the MDFN model for IMH status prediction. (D) The ROC curves of the VGG model for MH status prediction. (E) The ROC curves of the FCN model for MH status prediction. (F) The ROC curves of the VGG model for IMH status prediction. (G) The ROC curves of the FCN model for IMH status prediction. FCN, fully connected network; MDFN, multimodal deep fusion network; MH, macular hole; IMH, idiopathic macular hole; VGG, Visual Geometry Group.

integrates OCT image features and various clinical data of IMH to make an accurate prediction of postoperative IMH status.

Multimodal fusion of different sets of deep features has been proposed in previous studies. For instance, a multimodal DL model was developed for diagnosis of age-related macular degeneration (AMD). Two sets of deep features were extracted from colour fundus photographs and OCT images. After integrating

the two types of features, the DL model exhibited an AUC of 0.969.[26] In another study, the traditional handcrafted features and deep features of colour fundus photographs were integrated to detect hard exudates for diabetic retinopathy screening, with an AUC of 0.9323 and 0.9644 in two benchmark databases, respectively.[27] As mentioned before, the IMH status after surgery is affected by various factors, such as the preoperative
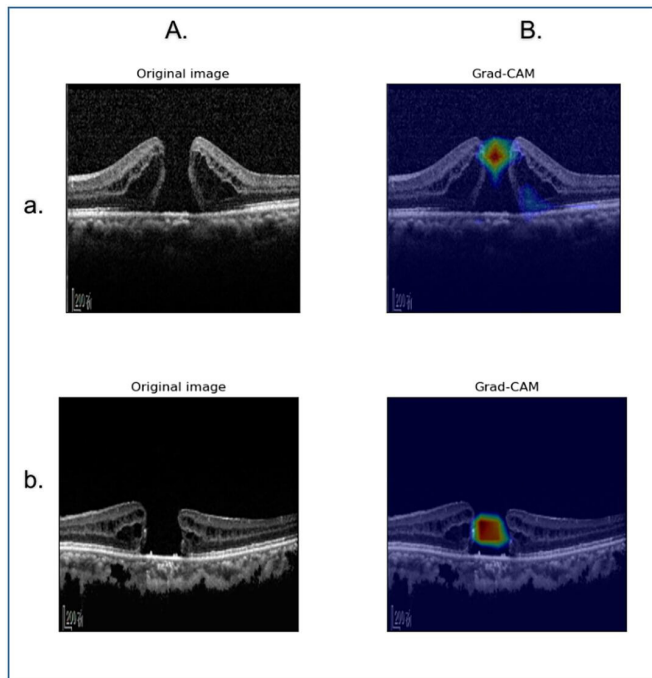
Figure 4 Visualisation heatmaps for prediction of the macular hole status after surgery. The heatmaps were generated by Gradient-weighted Class Activation Mapping (Grad-CAM). The heatmaps highlight the pathological area most important for accurate prediction of the macular hole status after surgery in optical coherence tomography images.

OCT morphology and other clinical data. For the information of OCT morphology, some could be virtually measured, while the others could be embedded in the OCT image and cannot be directly measured. It is important to integrate this information to obtain an accurate prediction of IMH status after surgery. Our MDFN model contains two modules, feature extraction and feature fusion. Two types of IMH deep features were extracted, including features of the preoperative macular OCT images extracted by VGG network and features of the clinical data extracted by FC network. These two sets of features were fused by the MDFN model to predict MH status after VILMP. The better prediction accuracy of the MDFN model than those of the unimodal DL models in our study indicated that DL models based on the fusion of multimodal feature sets have better prediction performance than DL models based on unimodal feature set. Consequently, the multimodal DL models are more suitable for prediction tasks with influencing factors from multiple feature sets. Since the prognosis of many ocular diseases such as IMH and AMD is affected by factors from different feature sets (eg, image and text), it is worth applying the multimodal DL models in further studies about prognosis prediction of these ocular diseases.

Multimodal fusion refers to the combination of multiple data sets in various forms (eg, image and text) to perform target prediction, which can exploit comprehensive information provided by multimodal data. Multimodal fusion typically occurs at the feature level. The advantage of feature-level fusion lies in two aspects. First, it can obtain the most discriminatory information from original feature sets. Second, it can eliminate the redundant information resulting from the correlation between different feature sets and make real-time decisions possible. In other words, feature fusion is capable of deriving and gaining the powerful and comprehensive features important for final prediction.[23 28]

Limitations

There are several limitations to this study, one of which is the relatively small sample size. However, the IMH eyes included in the study were from multiple ophthalmic centres, and the promising performance of the MDFN model was validated by an independent external dataset, suggesting that our MDFN model has excellent adaptability and generalisability. Another limitation is the manual measurements of preoperative macular OCT parameters, which are subject to measurement errors. Nevertheless, the repeatability and reproducibility of manual measurements on SD-OCT have been proved good in previous studies.[29 30] Recently, a fully automated 3D OCT image analysis of DL model has been developed for accurate measurement of MH parameters, which is potentially useful for automating MH measures in our DL models in the future.[31] Besides, this is a preliminary study to evaluate the possibility of predicting the postoperative IMH status using an MDFN model. Prospective multiple centre trials are needed to verify the accuracy of our MDFN model. Lastly, only a small number of eyes with SMH were included in the study, and we did not include eyes with SMH secondary to macular oedema or vitrectomy, as these patients were rarely seen in clinics. Further studies are needed to predict the postoperative status of SMH.

CONCLUSIONS

In conclusion, our DL-based models are highly accurate in classification of MH aetiology and prediction of postoperative MH/IMH status. The DL-based models are potentially useful to help make automatic diagnosis and better surgical planning for patients with MH.

Author affiliations
[1]Guangdong Eye Institute, Department of Ophthalmology, Guangdong Provincial People's Hospital, Guangdong Academy of Medical Sciences, Guangzhou, China
[2]Second School of Clinical Medicine, Southern Medical University, Guangzhou, China
[3]Aier Institute of Refractive Surgery, Refractive Surgery Center, Guangzhou Aier Eye Hospital, Guangzhou, China
[4]Aier School of Ophthalmology, Central South University, Changsha, China
[5]School of Computer Science and Engineering, South China University of Technology, Guangzhou, China
[6]State Key Laboratory of Ophthalmology, Zhongshan Ophthalmic CenterSun, Yat-sen University, Guangzhou, China
[7]Department of Opthalmology, the First Affiliated Hospital of Kunming Medical University, Kunming, China
[8]Department of Ophthalmology, Zhujiang Hospital of Southern Medical University, Guangzhou, China
[9]Center of Precision Medicine, Sun Yat-sen University, Guangzhou, China

Disclaimer The funders had no role in the design and conduct of the study; collection, management, analysis and interpretation of the data; preparation, review or approval of the manuscript and decision to submit the manuscript for publication.

Competing interests None declared.

Patient consent for publication Not required.

Ethics approval The study was conducted according to the Declaration of Helsinki and was approved by the Institutional Review Board of Guangdong Provincial People's Hospital (GPPH, No. GDREC2020067H). Informed consent was taken from all patients.

Provenance and peer review Not commissioned; externally peer reviewed.

Data availability statement Data are available on reasonable request (e-mail: yuhonghua@gdph.org.cn).

ORCID iDs
Yu Xiao http://orcid.org/0000-0002-0911-6857
Yijun Hu http://orcid.org/0000-0002-6424-7905
Qiaowei Wu http://orcid.org/0000-0002-3054-2682
Tao Li http://orcid.org/0000-0001-8064-871X
Haotian Lin http://orcid.org/0000-0003-4672-9721
Honghua Yu http://orcid.org/0000-0002-0782-346X

REFERENCES

1 Takahashi A, Yoshida A, Nagaoka T, *et al*. Idiopathic full-thickness macular holes and the vitreomacular interface: a high-resolution spectral-domain optical coherence tomography study. *Am J Ophthalmol* 2012;154:881–92. e882.

2 McCannel CA, Ensminger JL, Diehl NN, *et al*. Population-based incidence of macular holes. *Ophthalmology* 2009;116:1366–9.

3 Thapa SS, Thapa R, Paudyal I, *et al*. Prevalence and pattern of vitreo-retinal diseases in Nepal: the Bhaktapur glaucoma study. *BMC Ophthalmol* 2013;13:9.

4 Ali FS, Stein JD, Blachley TS, *et al*. Incidence of and risk factors for developing idiopathic macular hole among a diverse group of patients throughout the United States. *JAMA Ophthalmol* 2017;135:299–305.

5 Duker JS, Kaiser PK, Binder S, Susanne B, *et al*. The International Vitreomacular traction Study Group classification of vitreomacular adhesion, traction, and macular hole. *Ophthalmology* 2013;120:2611–9.

6 Chew EY, Sperduto RD, Hiller R, *et al*. Clinical course of macular holes: the eye disease case-control study. *Arch Ophthalmol* 1999;117:242–6.

7 Gross JG, Gross Jeffrey G. Late reopening and spontaneous closure of previously repaired macular holes. *Am J Ophthalmol* 2005;140:556–8.

8 Yao Y, Qu J, Dong C, *et al*. The impact of extent of internal limiting membrane peeling on anatomical outcomes of macular hole surgery: results of a 54-week randomized clinical trial. *Acta Ophthalmol* 2019;97:303–12.

9 Abbey AM, Van Laere L, Shah AR, *et al*. Recurrent macular holes in the era of small-gauge vitrectomy: a review of incidence, risk factors, and outcomes. *Retina* 2017;37:921–4.

10 Michalewska Z, Michalewski J, Adelman RA, *et al*. Inverted internal limiting membrane flap technique for large macular holes. *Ophthalmology* 2010;117:2018–25.

11 Valldeperas X, Wong D. Is it worth reoperating on macular holes? *Ophthalmology* 2008;115:158–63.

12 Lin C-W, Ho T-C, Yang C-M. The development and evolution of full thickness macular hole in highly myopic eyes. *Eye* 2015;29:388–96.

13 Tang YF, Chang A, Campbell WG, *et al*. Surgical management of traumatic macular hole: optical coherence tomography features and outcomes. *Retina* 2020;40:290–8.

14 Wu T-T, Kung Y-H, Chang C-Y, *et al*. Surgical outcomes in eyes with extremely high myopia for macular hole without retinal detachment. *Retina* 2018;38:2051–5.

15 Wakely L, Rahman R, Stephenson J. A comparison of several methods of macular hole measurement using optical coherence tomography, and their value in predicting anatomical and visual outcomes. *Br J Ophthalmol* 2012;96:1003–7.

16 Ip MS, Baker BJ, Duker JS, *et al*. Anatomical outcomes of surgery for idiopathic macular hole as determined by optical coherence tomography. *Arch Ophthalmol* 2002;120:29–35.

17 Ullrich S, Haritoglou C, Gass C, *et al*. Macular hole size as a prognostic factor in macular hole surgery. *Br J Ophthalmol* 2002;86:390–3.

18 Kusuhara S, Teraoka Escaño MF, Fujii S, *et al*. Prediction of postoperative visual outcome based on hole configuration by optical coherence tomography in eyes with idiopathic macular holes. *Am J Ophthalmol* 2004;138:709–16.

19 Ruiz-Moreno JM, Staicu C, Piñero DP, *et al*. Optical coherence tomography predictive factors for macular hole surgery outcome. *Br J Ophthalmol* 2008;92:640–4.

20 Kermany DS, Goldbaum M, Cai W, *et al*. Identifying medical diagnoses and treatable diseases by image-based deep learning. *Cell* 2018;172:e1129:1122–31.

21 Liu H, Li L, Wormstone IM, *et al*. Development and validation of a deep learning system to detect glaucomatous optic neuropathy using fundus Photographs. *JAMA Ophthalmol* 2019;137:1353.

22 Nagasawa T, Tabuchi H, Masumoto H, *et al*. Accuracy of deep learning, a machine learning technology, using ultra-wide-field fundus ophthalmoscopy for detecting idiopathic macular holes. *PeerJ* 2018;6:e5696.

23 Jingdong W, Zhen W, Ting Z. Deeply-fused nets. *arXiv* 2016.

24 Rawat W, Wang Z, Waseem R. Deep convolutional neural networks for image classification: a comprehensive review. *Neural Comput* 2017;29:2352–449.

25 Morizane Y, Shiraga F, Kimura S, *et al*. Autologous transplantation of the internal limiting membrane for refractory macular holes. *Am J Ophthalmol* 2014;157:861–9. e861.

26 Yoo TK, Choi JY, Seo JG, *et al*. The possibility of the combination of OCT and fundus images for improving the diagnostic accuracy of deep learning for age-related macular degeneration: a preliminary experiment. *Med Biol Eng Comput* 2019;57:677–87.

27 Wang H, Yuan G, Zhao X, *et al*. Hard exudate detection based on deep model learned information and multi-feature joint representation for diabetic retinopathy screening. *Comput Methods Programs Biomed* 2020;191:105398.

28 Ke L, Changqing Z, Shuhui B. Multi-modal feature fusion for geographic image annotation. *Pattern Recognit* 2018;73:1–14.

29 Rahman W, Chen FK, Yeoh J, *et al*. Repeatability of manual subfoveal choroidal thickness measurements in healthy subjects using the technique of enhanced depth imaging optical coherence tomography. *Invest Ophthalmol Vis Sci* 2011;52:2267–71.

30 Chhablani J, Barteselli G, Wang H, *et al*. Repeatability and reproducibility of manual choroidal volume measurements using enhanced depth imaging optical coherence tomography. *Invest Ophthalmol Vis Sci* 2012;53:2274–80.

31 Murphy DC, Nasrulloh AV, Lendrem C, *et al*. Predicting postoperative vision for macular hole with automated image analysis. *Ophthalmol Retina* 2020;4:1211–3.